SP-356—2

Numerical Investigation on Mechanical Splices for GFRP Reinforcing Bars

Nafiseh Kiani, Steven Nolan, and Antonio Nanni

Synopsis: A common challenge in reinforced concrete construction is the need to connect bars of finite length to provide reinforcement continuity. Lap and mechanical splices are common methods that have been used to make a continuous reinforcement. Lap splicing may cause additional congestion making the concrete consolidation difficult. Mechanical splices are used when lap splicing is not practical. Different types of mechanical splices are commercially available for steel bars. For the case of GFRP reinforcement, mechanical splices are very useful in staged construction because the reinforcement cannot either be bent at the site or there is insufficient space for lap splicing. Mechanical splices for GFRP bars, however, must account for the low transverse stiffness and strength of the bars. For these reasons, only certain mechanical splices are practical for GFRP bars and careful consideration must be given to their installation and effectiveness. In this study, a commercially available swaged coupler was selected to investigate the behavior of spliced GFRP bars. Expected performance was numerically evaluated using a Finite Element (FE) model to develop a framework for test validation. The FE model was calibrated with a laboratory test to compare the results. The coupler's length, bar's tensile strength, and slip between the coupler and bar were investigated. The outcome of this study allows for the definition of an efficient test campaign.

Keywords: GFRP bars; Mechanical splice; Swaged coupler; Finite Element Model.

ACI member **Nafiseh Kiani** received her PhD degree in Civil Engineering from University of Miami in 2022. Her research is mainly focusing on mechanical splices for FRP reinforcing bars in concrete structures to address the challenges of splicing FRP bars.

ACI member **Steven Nolan** is a practicing engineer with the Florida Department of Transportation. In his 25 years with FDOT, he has worked primarily in highway bridge design and assisted in development of many of the related FDOT Structures Standards. He is a member of the Transportation Research Board's AKB10 Standing Committee on Innovative Highway Structures and Appurtenances; Bridge Engineering Institute's Scientific Advisory Panel; and a reviewer for several engineering journals.

ACI member **Antonio Nanni**, Professor of Civil Engineering at the University of Miami, has research interests in construction materials, their structural performance and their field application. His research in materials and structures has impacted the work of technical committees in the US and abroad including professional and standards-writing agencies such as AASHTO, ACI, ASCE, ASTM and ICC-ES.

INTRODUCTION

In reinforced concrete (RC) structures, corrosion of steel reinforcement can result in high repair costs. Fiber-reinforced polymer (FRP) bars are known as alternatives to eliminate the corrosion problem in aggressive environments and coastal structures[1,2]. The mechanical properties of FRP bars differ from steel bars. Compared to steel bars, they have anisotropic properties with higher longitudinal tensile strength, lower transverse strength, lower modulus of elasticity, greater durability, and elastic behavior up to rupture. Among different FRP composites, Glass FRP (GFRP) bars are commonly specified for their efficient cost to performance ratio[3]. GFRP bars using a thermoset resin as a matrix present some constructability challenges because they cannot be bent after the resin is polymerized. FRP is anisotropic; thus, the strength in the transverse (resin-dominated) direction is significantly lower than those in the longitudinal (fiber-dominated) direction.

FRP bars typically require longer development lengths than steel bars due to a lower bond strength to tensile strength ratio [4,5]. Studies on the bond behavior of FRP bars are continuing [6], and recent works have focused on improving the bond performance and structural response of FRP composites in different concrete elements [7,8]. Because of the lack of bendability and requiring a longer development length in lap splicing, FRP bars present a significant challenge in terms of constructability when a bar needs to be spliced. One of the gaps in FRP-RC construction is the need to connect bars with mechanical splices in order to provide reinforcement continuity.

Lap and mechanical splicing are two standard methods that are used for splicing reinforcing bars. The lap splice is a common method because of its inexpensive and simple installation [9]. However, lap splices are not practical in many applications. For example, lap splices are not permitted for steel bars larger than No.11 bars according to ACI 318. Lap splices must be enclosed within stirrups, ties, or spirals to prevent the failure of lap splice. For large bar sizes and epoxy-coated bars, long lap splice lengths based on code requirements can cause congestion at splice locations [10]. In such cases, mechanical splices are preferable. Mechanical splices are used for cast-in-place or precast concrete members when long and continuous reinforcement is required[11]. Mechanical splices are applicable for construction joints to provide tensile continuity for future construction, minimize formwork penetrations, or minimize the work zone footprint for staged construction[12]. The use of mechanical splices may reduce the amount of longitudinal reinforcement in splice regions to satisfy a steel ratio of a maximum of 8% for reinforced concrete columns [13]. Mechanical splices are desirable for both rehabilitation and new construction where reinforcements must be spliced to existing bars[14,15].

Mechanical splices are also referred to as couplers, consist of a coupling sleeve to connect two bars for directly transferring tension or compression. There are different types of mechanical splices for steel bars that are commercially available (Figure 1). Swaged couplers, threaded couplers, shear screw couplers, and grouted sleeve couplers are typical couplers employed in structural members. Swaged couplers are compatible with the low transverse strength and non-malleable nature of GFRP bars. However, limited experimental studies are available on the behavior of swaged couplers [16]. Swaged couplers are installed by deforming a steel coupler onto two bar ends using a hydraulic press and a series of overlapping pressings.

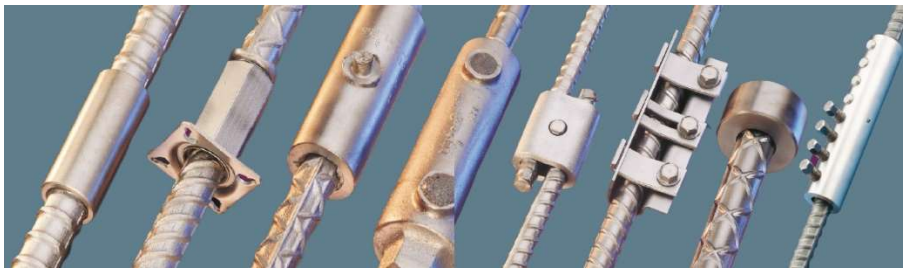

Figure 1. Different types of mechanical couplers for steel bars

Mechanical splices are classified into two types: Type 1 splices to transfer tension or compression (full mechanical splices) in members where inelastic deformations may result from seismic events. According to ACI 318, Type 1 splices are required to meet a minimum of 125% of the steel bar's specified yield strength (1.25 f_y). Type 2 splices transfer only compression forces (compression-only or end-bearing splices), thus, are required to satisfy the ultimate tensile strength of steel bars (1.0 f_u). Because of these limitations, seismic design specifications prohibit using mechanical couplers in plastic hinge regions of columns in the seismic areas[17]. Recent studies have been conducted to identify suitable mechanical couplers for precast concrete columns [18].

For steel bars, design codes develop acceptance requirements to resist slippage, transfer the load, and avoid splice failure before the bar reaches its ultimate tensile strength. AC133 and ACI 439 are available documents to address performance requirements and details of mechanical splices[19,20]. Standard test methods for testing the mechanical splices for steel bars are specified based on ASTM A1034[21]. In the United States, some state Departments of Transportation (DOTs) have developed their own requirements for spliced steel bars[22]. The coupler's ultimate strength varies for each bar size and depends on the coupler's mechanical properties, the coupler's length, and the stress on the bar. Tensile and slip tests are two acceptable tests to determine the coupler's ultimate strength and displacement across the coupler, respectively[23]. According to ACI 318, there are no criteria regarding the mechanical splice's dimensions and the coupler's length. Most manufacturers assume $8d_b$ for No.3 to No.5 bars and $7d_b$ for No.6 and larger steel bars (where d_b is the bar diameter*)*. For steel bars, the California Department of Transportation test method requires a coupler's length less than ten times the nominal bar diameter[22].

For GFRP bars, no requirements regarding the mechanical splices are available in ACI 440 or AASHTO GFRP[24,25]. This is recognized to be a major limitation to the full deployment of this technology as it imposes significant challenges to constructability. A research project was, thus, initiated in order to provide a contribution towards the development of knowledge on the performance of mechanical splices for GFRP bars. This study initially considered commercially available swaged couplers for splicing No.4 GFRP bars. This type of coupler was identified to be the ideal candidate for splicing GFRP bars since it applies a controllable pressure on bar terminations and could be potentially made of stainless steel or other corrosion-resistant metal to maintain durability. Accordingly, a preliminary study showed that swaged couplers were effective in the field for splicing GFRP to GFRP bars or GFRP bars to steel strands [26].

After some proof-of-concept experimental tests, this research proceeded with a numerical simulation of the GFRP bar-coupler system. This Finite Element (FE) simulation was intended to assess the criticality of the following variables: swaging pressure on the GFRP bar and coupler's length. Based on the outcome of this numerical study, a test matrix was developed for an experimental campaign aimed at validating performance.

RESEARCH SIGNIFICANCE

To develop the field-deployable application of GFRP bars, structural integrity reinforcement requirements in continuous members need to be satisfied. When the length of the GFRP bar is limited due to logistic considerations or where work-zone geometric constraints or reinforcing congestion preclude lap splicing, then mechanical splices are the best alternatives. Thus, the lack of an efficient mechanical splice that can be easily installed at a factory or using inexpensive portable equipment in the field while matching the non-corrosive nature of GFRP creates a significant barrier to the deployment of composite reinforcement. This research develops a numerical study focusing on steel swaged couplers for splicing No.4 GFRP bars to partially fill the knowledge gap concerning mechanical splices for GFRP bars.

PARAMETRIC STUDY

This study investigates the effect of the swaging pressure and coupler's length on the load-displacement behavior of spliced GFRP bars. Three swaging pressure values and three coupler lengths were considered in this study. The behavior of GFRP bars under transverse loading is mostly influenced by the properties of the resin matrix (vinyl ester). Thus, the compressive strength of the vinyl ester (VE) resin is used as the criteria for residual stresses on the GFRP bar after the swaging pressure to avoid crushing the bar. The minimum VE compressive strength is assumed to be 82 MPa, and the average value is assumed 215 MPa[27,28]. It is possible that experimental results may demonstrate that a GFRP bar can resist much higher transverse pressure being in a state of full confinement. In this study, two No.4 GFRP bars were spliced using a swaged coupler. Then, a FE model was developed and calibrated with experimental results obtained from a tension test. The validated FE model was used to investigate the pressure on the GFRP bar and coupler's length parameters. Three coupler lengths of $8d_b$, $10d_b$, and $12d_b$ were used for No.4 GFRP bars to study the effect of the coupler's length on the load-displacement behavior of the spliced bars.

SPECIMEN DETAILS

Swaged couplers were selected to investigate splicing No.4 GFRP bars. The coupler was made of a low carbon steel grade 1020 according to ASTM A519. The coupler has uniform inside and outside diameters around the length of the bar, as shown in Figure 2. GFRP bars were inserted halfway into each end of the coupler, and a hydraulic press was used to swage the coupler. The steel coupler was plastically deformed onto the bars to produce a mechanical interlock resulting from the residual pressure. Figure 3 shows two sand-coated No.4 GFRP bars spliced with a swaged coupler.

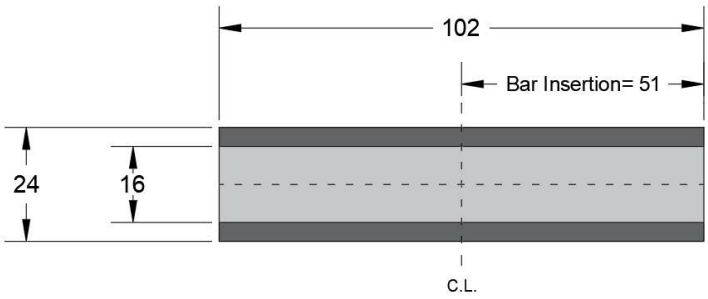

Figure 2. Swaged coupler before swaging (dimensions are in mm)

Figure 3. Spliced GFRP bars with swaged coupler

FINITE ELEMENT MODEL

A detailed FE model was developed in ABAQUS to simulate the performance of spliced GFRP bars with the swaged coupler. Three-dimensional eight-node linear brick elements were used for both the GFRP bar and the coupler. The GFRP material was modeled using its anisotropic properties shown in Table 1. The steel coupler is considered isotropic with elastic-plastic hardening behavior and yield strength of 264 MPa. The plastic deformation behavior of the steel was defined using the true stress-strain curve [29].

Table 1. The material properties of GFRP bar and coupler in FEM

Property	Value	Unit
GFRP bar		
Longitudinal modulus (E_1)	45	
Transverse modulus (E_2)	10	GPa
Transverse modulus (E_3)	10	
Poisson's ratio (ν_{12})	0.27	
Poisson's ratio (ν_{13})	0.27	
Poisson's ratio (ν_{23})	0.40	
Shear modulus (G_{12})	4.0	
Shear modulus (G_{13})	4.0	GPa
Shear modulus (G_{23})	3.6	
Steel coupler		
Young's modulus	200	GPa
Yield strength	264	MPa
Poisson's ratio	0.3	

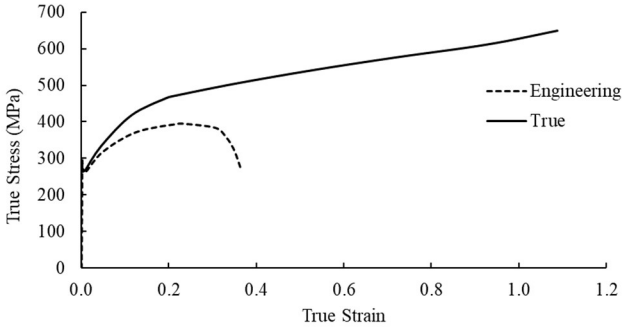

Figure 4. Stress-strain curve of steel coupler

For boundary conditions, the coupler was assumed Symmetry in the direction of the bar. The swaging process was simulated by modeling two dies to press the coupler onto the GFRP bars, as shown in Figure 5. Three load steps were considered in the FE model. First, the swaging pressure was applied on the steel coupler to reach all elements' yield strength and obtain the specified residual stress on the bar. Second, the swaging pressure was removed, while residual stresses resulting from mechanical swaging remained on the bar (Figure 5). Third, a uniform linear displacement load was applied to the end of the bar to pull out the bar from the deformed coupler. The coupler's maximum slip resistance was obtained from load-displacement curves for each parameter.

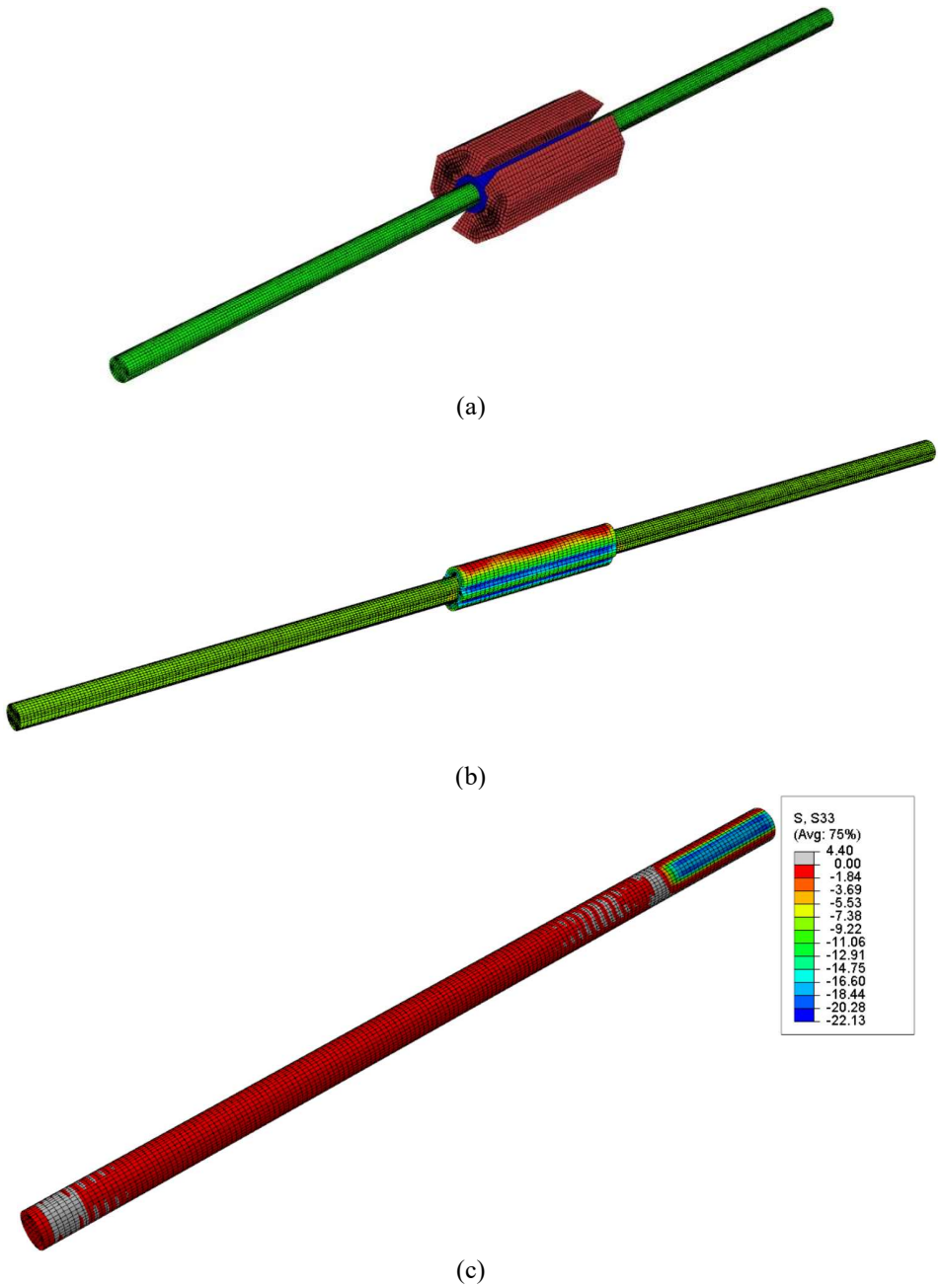

Figure 5. FE model for $8d_b$ long coupler: (a) Swaging; (b) Deformed coupler after swaging; (c) Residual stresses on the bar after swaging (contour units in ksi; 1 ksi= 6.89 MPa)

RESULTS AND DISCUSSION

The FE model is used for parametric analyses on spliced No.4 GFRP bars, and the numerical results are discussed and plotted for this bar size. The FE model was calibrated using experimental data obtained from a tension test performed on spliced No.4 GFRP bars with an $8d_b$ long swaged coupler according to ASTM D7205[30]. The load-displacement curves resulting from the tension test and the FEM are shown in Figure 6. It can be seen that FEM results showed a good agreement with experimental results. The tension test results showed that GFRP bars spliced with a coupler length of $8d_b$ reached 22% of the bar's guaranteed ultimate tensile load. Moreover, the slip occurred at 18% of the bar's guaranteed ultimate tensile load. The validated FE model is used to investigate the splice capacity for three coupler lengths and estimate the residual stress on the GFRP bar. The load-displacement curves for three coupler lengths (i.e., $8d_b$, $10d_b$, and $12d_b$) were obtained from the FE model and plotted in Figure 7.

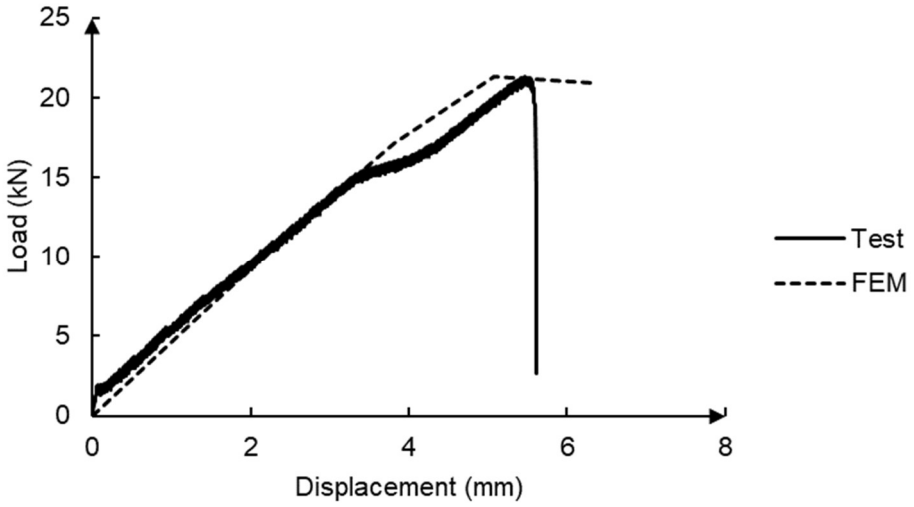

Figure 6. Comparison of load-displacement curves obtained from test and FEM for $8d_b$ long coupler

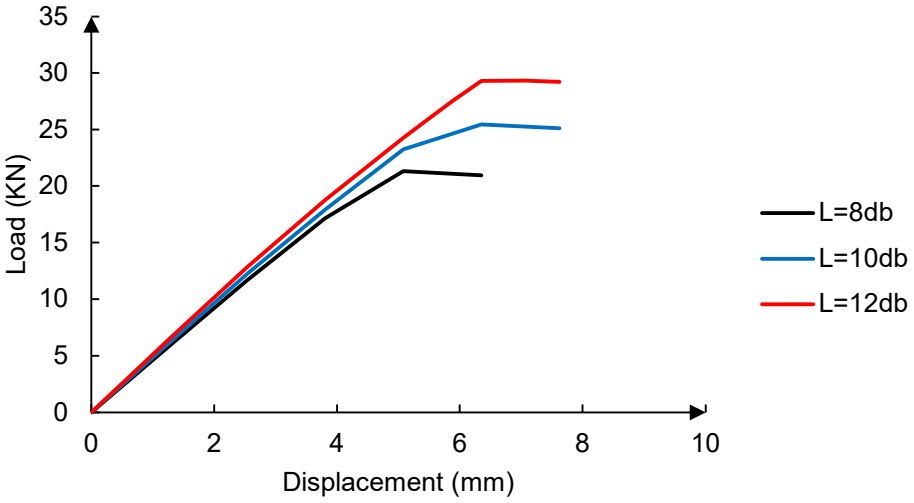

Figure 7. Load-displacement curves for different coupler lengths using 166 MPa residual pressure

The FE results showed that the coupler's slip resistance is affected by the swage pressure that results in corresponding residual stresses on the bar. The load-slip behavior appears to be almost linear up to about the maximum value of the load; then, slips progresses without load increasing. The reason is that the radial stresses in the coupler have already reached the yield strength; thus, increasing the swage pressure does not increase the contact pressure on the bar and only causes additional plastic deformation within the coupler. In addition, as the coupler's length is increased from $8d_b$ to $10d_b$ and $12d_b$, the slip resistance increases by 19% and 38%, respectively (Figure 7). Moreover, the FE results showed that the coupler's maximum slip resistance is dependent to stresses on the GFRP bar. The slip load values (P_s) are shown in Table 2. The maximum loads are presented as a ratio of minimum guaranteed ultimate tensile force of the bar according to ASTM D7957[31]. The FE results showed that to reach more than 22% of the bar's guaranteed ultimate tensile force as obtained from test results, the coupler's length has to be more than $12d_b$. The residual stress values didn't show significant changes by increasing swaging pressure. The validated FE model is used to estimate

the residual pressure on the GFRP bar after the swaging. Based on calibrated FEM, the residual pressure on No.4 GFRP bars spliced with the $8d_b$ long coupler was 166 MPa after swaging.

Table 2. The FE results for spliced GFRP bars with swaged coupler

Bar Size	Deformation	Coupler Length	Swage Pressure on GFRP (MPa)	Residual Pressure on GFRP (MPa)	P_s (KN)	Slip at P_s (mm)	P_s/GUS* (%)
#4	Sand	$8d_b$	362	166	21.3	5.1	22%
			695	216	44.5	10.2	46%
			861	219	61.8	15.2	64%
		$10d_b$	362	166	25.5	6.4	27%
			701	209	53.1	11.4	55%
			853	213	72.7	15.9	76%
		$12d_b$	362	85	29.3	7.1	31%
			642	181	60.4	12.7	63%
			1070	244	79.9	17.8	83%

Note: GUT* = Minimum Guaranteed Ultimate Tensile Force (96 KN according to ASTM D7957)

FUTURE RESEARCH

The FE model has to be validated using more experimental test results. The tensile behavior of spliced GFRP bars considering the mentioned parameters needs to be evaluated through static tensile tests specified in ASTM D7205. The laboratory tests are under investigation to complete this parametric study. Furthermore, additional bar sizes up to #8 (25 mm) GFRP bar will be investigated in future work.

CONCLUSIONS

The availability of a mechanical coupler that allows for the continuity of GFRP bars is a significant challenge for the construction of heavily reinforced concrete structures as well as staged construction due to the inability to bend bars in the field. In this study, a swaged coupler was selected to investigate the feasibility of splicing GFRP bars. A FE model was developed and calibrated with experimental results to evaluate the effect of swaging pressure and coupler's length on the load-displacement behavior of spliced GFRP bars. Three swaging pressures and three coupler lengths were considered as key parameters. The compressive strength of the resin matrix was used to gauge the residual stresses on the GFRP bar. The validated FE model is used to estimate the residual pressure on the GFRP bar after swaging and the slip resistance of the coupler. The load-displacement curves for spliced GFRP bars were obtained. Based on the numerical results, the coupler's slip resistance is dependent to residual stress on the bar. It was observed that the effect of the coupler's length is significant to increase the splice capacity. For example, to achieve more than 30% of the bar's guaranteed ultimate strength, the coupler length must be more than $12d_b$ for No.4 GFRP bars. The validated FE model of this study will allow researchers to find the swaged coupler's approximate slip and expected slip load for a variety of parameters.

ACKNOWLEDGMENTS

The authors gratefully acknowledge the financial support from "CICI: Center for the Integration of Composites into Infrastructure" National Science Foundation, I/UCRC:1439543.

REFERENCES

1. Hansson, C. M. "The impact of corrosion on society," *Metallurgical and Materials Transactions A: Physical Metallurgy and Materials Science*, V. 42, No. 10, 2011, pp. 2952–62.
2. Ghiasian, M., Rossini, M., Amendolara, J., Haus, B., Nolan, S., Nanni, A., Bel Had Ali, N., and Rhode-

Barbarigos, L. "Test-driven design of an efficient and sustainable seawall structure," *Coastal Structures 2019*, 2019, pp. 1222–7.
3. Cadenazzi, T., Dotelli, G., Rossini, M., Nolan, S., and Nanni, A. "Cost and environmental analyses of reinforcement alternatives for a concrete bridge," *Structure and Infrastructure Engineering*, V. 0, No. 0, 2019, pp. 1–16.
4. Elnemr, A., Ahmed, E., Barris, C., and Benmokrane, B. "Bond-dependent coefficient of glass- and carbon-FRP bars in normal- and high-strength concretes," *Construction and Building Materials*, V. 113, 2016, pp. 77–89.
5. Rolland, A., Quiertant, M., Khadour, A., Chataigner, S., Benzarti, K., and Argoul, P. "Experimental investigations on the bond behavior between concrete and FRP reinforcing bars," *Construction and Building Materials*, V. 173, 2018, pp. 136–48.
6. Tabatabaei, A., Eslami, A., Mohamed, H. M., and Benmokrane, B. "Strength of compression lap-spliced GFRP bars in concrete columns with different splice lengths," *Construction and Building Materials*, V. 182, 2018, pp. 657–69.
7. Zhang, B., Zhu, H., Wu, G., Wang, Q., and Li, T. "Improvement of bond performance between concrete and CFRP bars with optimized additional aluminum ribs anchorage," *Construction and Building Materials*, V. 241, No. January, 2020, p. 118012.
8. Farhangi, V., and Karakouzian, M. "Effect of fiber reinforced polymer tubes filled with recycled materials and concrete on structural capacity of pile foundations," *Applied Sciences (Switzerland)*, V. 10, No. 5, 2020.
9. Aly, R., Benmokrane, B., and Ebead, U. "Tensile lap splicing of fiber-reinforced polymer reinforcing bars in concrete," *ACI Structural Journal*, V. 103, No. 6, 2006, pp. 857–64.
10. ACI Committee 318. "Building Code Requirements for Structural Concrete (ACI 318-19)," *American Concrete Institute*, 2019.
11. Khedmatgozar Dolati, S. S., and Mehrabi, A. "Review of available systems and materials for splicing prestressed-precast concrete piles," *Structures*, V. 30, 2021, pp. 850–65.
12. Jansson, P. O. "Evaluation of Grout-Filled Mechanical Splices for Precast Concrete Construction," *Michigan Department of Transportation*, 2008.
13. ACI Committee 439. "Types of Mechanical Splices for Reinforcing Bars (ACI 439.3R-07)," *American Concrete Institute*, 2007, p. 20.
14. Haber, Z. B., Saiid Saiidi, M., and Sanders, D. H. "Behavior and simplified modeling of mechanical reinforcing bar splices," *ACI Structural Journal*, V. 112, No. 2, 2015, pp. 179–88.
15. Valikhani, A., Jahromi, A. J., Mantawy, I. M., and Azizinamini, A. "Effect of mechanical connectors on interface shear strength between concrete substrates and UHPC: Experimental and numerical studies and proposed design equation," *Construction and Building Materials*, V. 267, 2021, p. 120587.
16. Jordan, E. J., and Saiidi, M. "Experimental Studies of Reinforcing Steel and Shape Memory Alloys in Mechanically Spliced Connections for Seismic Application," *MSc Thesis*, 2018.
17. AASHTO. "AASHTO Guide Specifications for LRFD Seismic Bridge Design," *American Association of State Highway and Transportation Officials*, 2011.
18. Tazarv, M., and Saiidi, M. S. "Seismic design of bridge columns incorporating mechanical bar splices in plastic hinge regions," *Engineering Structures*, V. 124, 2016, pp. 507–20.
19. International Code Council Evaluation Service (ICC-ES). "Acceptance Criteria for Mechanical Connector Systems for Steel Reinforcing Bars (AC133)," 2010.
20. ACI Committee 439. "Types of Mechanical Splices for Reinforcing Bars (ACI 439.3R-07)," Farmington Hills, MI, 2007.
21. ASTM A1034. "Standard Test Methods for Testing Mechanical Splices for Steel Reinforcing Bars (ASTM A1034)," *ASTM International*, 2015.
22. California Test 670. "Method of Tests for Mechanical and Welded Reinforcing Steel Splices," *California Department of Transportation*, 2011.
23. ASTM A370. "Standard Test Methods and Definitions for Mechanical Testing of Steel Products (A370)," *ASTM International*, 2020.
24. ACI Committee 440. "Guide for the Design and Construction of Structural Concrete Reinforced with Fiber-Reinforced Polymer Bars (ACI 440.1R-15)," *American Concrete Institute*, 2015.
25. AASHTO. "AASHTO LRFD Bridge Design Guide Specifications for GFRP-Reinforced Concrete, Second Edition," *American Association of State Highway and Transportation Officials*, 2018.
26. Kiani, N., Rossini, M., and Nanni, A. "Characterization of GFRP bars and couplers for prestressed concrete," *Composites and Advanced Materials Expo, CAMX 2020*, 2020.

27. Wypych, G. "Handbok of Polymers," *ChemTec Publishing*, 2012.
28. Stockton, S. L. "Engineering and Design: Composite Materials for Civil Engineering Structures," *Department of the Army U.S. Army Corps of Engineers*, 1997.
29. Abedin, M., Maleki, S., Kiani, N., and Shahrokhinasab, E. "Shear Lag Effects in Angles Welded at Both Legs," *Advances in Civil Engineering*, V. 2019, 2019, p. 8041767.
30. ASTM D7205/D7205M. "Standard Test Method for Tensile Properties of Fiber Reinforced Polymer Matrix Composite Bars," *ASTM International*, 2021.
31. ASTM D7957/D7957M. "Standard Specification for Solid Round Glass Fiber Reinforced Polymer Bars for Concrete Reinforcement," *ASTM International*, 2017.